

Adaptive PID control system for underactuated flying object through model-based prediction

Akira Yanou¹, Mamoru Minami¹ and Takayuki Matsuno¹

¹Graduate School of Natural Science and Technology, Okayama University, Japan
(Tel: +81-86-251-8924; E-mail: yanou-a@cc.okayama-u.ac.jp)

Abstract: This paper explores adaptive PID control system for an underactuated flying object through model-based prediction. Helicopter is applied in large field because of flight ability such as vertical ascent, vertical descent and hovering. However the helicopter, which is one of the underactuated flight objects, is complex and has nonlinear dynamics. In this research, controlled target is an underactuated flight object with two inputs and three outputs. The proposed method predicts the system outputs using the model of controlled target, and the control inputs are calculated by using their values. That is, PID control gains are adaptively changed at each control period by the model-based controlled result with time passing virtually. The control gains consist of switching part and fixed part in order to tune the control performance. An experimental result is shown to consider the effectiveness of the proposed method.

Keywords: Prediction, Underactuated flying object, Switching control

1. INTRODUCTION

Helicopter has been applied in large field because of flight ability such as vertical ascent, vertical descent and hovering. Manned helicopter is used for rescue, emergency activity and fire fighting at the time of disaster, and unmanned helicopter, such as drone, is precious sources of information in the danger spot where people cannot approach. On the other hand, the operation of helicopter is complex and sensitive to the influence of the wind. In order to challenge autonomous control operation, our laboratory manufactured an experimental device of three degree-of-freedom underactuated flying object[1]. This device can control roll, pitch and yaw angles by thrust gained by two rotors. Controlling an underactuated flying object has attracted a lot of attention, due to the fact that flying object is an underactuated nonlinear system. That is, it may be possible to contribute for reducing weight, lowering the cost, and the energy saving if the system can be controlled with the number of control inputs less than the number of outputs. We have been controlling three outputs using interference of roll angle through PID control[2] and combined control[3, 4], in their researches the prediction of the flying object has not been considered for its control. PID with fixed control gains is simple and the tuning method such as Ziegler-Nichols' ultimate gain method is well known, but it seems to be insufficient for nonlinear system. Although combined control is seemed to be appropriate for the system, the derived controller is complicated. Moreover, switching PID control method through model-based prediction has been also considered for the underactuated flying object model[5]. Therefore this paper applies an adaptive PID controller consisting of switching gains[5] and fixed ones to the experimental device and shows the experimental result to consider the practical ability of the proposed method. The model-based prediction to settle PID control gains is executed virtually in the control period. Because the number of predictions in the virtual time, which affects computation

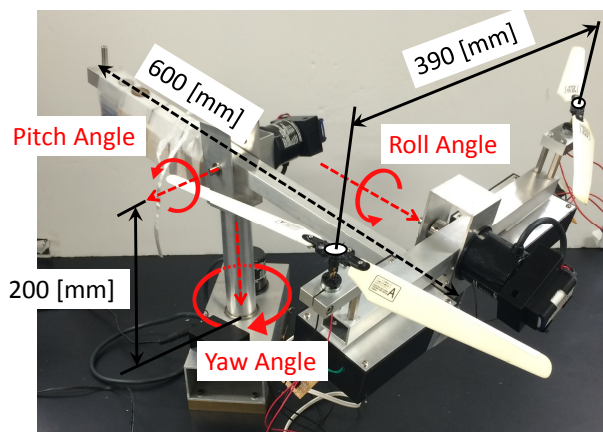


Fig. 1 Underactuated flying object

time, is given by the prediction horizon and the virtual sampling time, the proposed method depends on computer performance such as CPU frequency if long-range prediction horizon and virtual short sampling time are given. This paper is organized as follows. Section 2 models the underactuated flying object of our experimental system. Section 3 shows the concept of adaptive PID control through model-based prediction. Section 4 gives an experimental result in order to consider the effectiveness of proposed method. Section 5 concludes this paper.

2. MODELING

Controlled target shown in Fig. 1 is three degree-of-freedom underactuated flying object. The system has two inputs and three outputs, and attaches motors for rotating left and right rotor. Rotary encoders are installed for detecting roll, pitch and yaw angles. To avoid the controlled object from spinning by rotor drag torque, rotation of right rotor is the reverse rotation of left one. The equation of motion of three degree-of-freedom underactuated

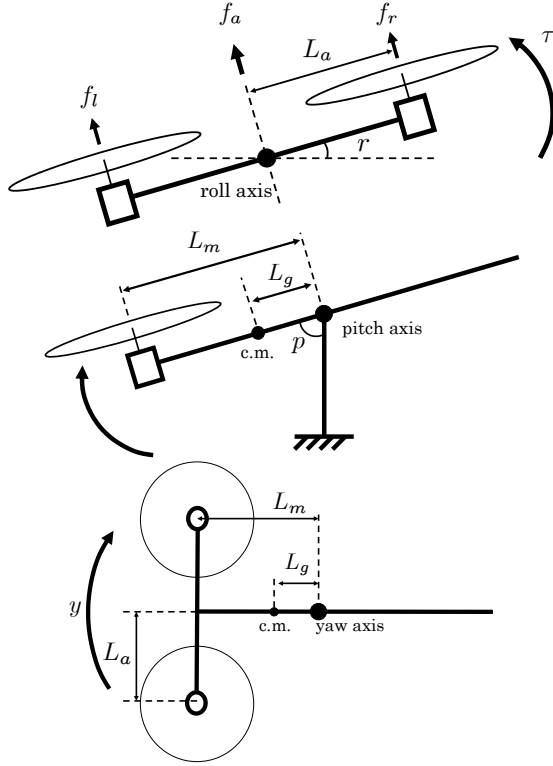


Fig. 2 Roll, pitch and yaw directions

flying object is given as follows.

Direction of the roll angle:

$$I_r \ddot{r} + D_r \dot{r} = \tau \quad (1)$$

Direction of the pitch angle:

$$I_p \ddot{p} + D_p \dot{p} + mgL_g \sin p = L_m f_a \cos r \quad (2)$$

Direction of the yaw angle:

$$I_y \ddot{y} + D_y \dot{y} = L_m f_a \sin r \quad (3)$$

Where r , p and y are angles of each direction, m is the system weight, g is gravity acceleration, I_r , I_p and I_y are moments of inertia of each direction, D_r , D_p and D_y are friction coefficients of each direction, L_m is distance from pitch axis to roll link and L_g is distance from pitch axis to center of mass. f_a means a resultant force of f_l and f_r , τ is a moment of roll direction.

$$\begin{aligned} f_a &= f_r + f_l \\ \tau &= L_a(f_l - f_r) \end{aligned} \quad (4)$$

f_r and f_l are the thrusts of right rotor and left one respectively. L_a is length from roll axis to the motor. The relation between rotor thrust and input voltage can be expressed as follows.

$$\begin{aligned} f_r &= \omega_r^2 A = A(ku_r)^2 = Ak^2 u_1 \\ f_l &= \omega_l^2 A = A(ku_l)^2 = Ak^2 u_2 \end{aligned} \quad (5)$$

ω_r and ω_l are the angular velocities of right and left rotor, A is a coefficient depending on the shape of rotor, u_r and

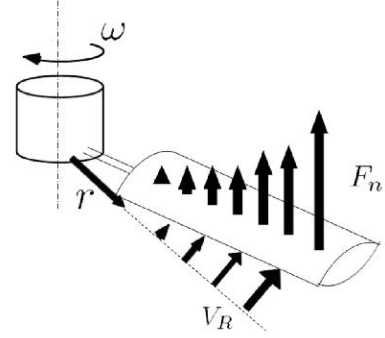


Fig. 3 Forces which act on the face of rotor

u_l are the input voltages to right and left motor, k is a coefficient between voltage and angular velocity, where $\omega_r = ku_r$ and $\omega_l = ku_l$. The equation of aerodynamical forces is considered by using the rotor angular velocity. And aerodynamical force in microscopic area is given as follows.

$$F_n = \frac{1}{2} \rho V_R^2 S C_z \quad (6)$$

$$V_R = \omega r \quad (7)$$

F_n is aerodynamical force in microscopic area, ρ is air-density, V_R is airspeed, S is surface area of the rotor, C_z is a coefficient of aerodynamical forces and r is distance from shaft. F_n is a function of r as shown in Fig. 3. Air-density ρ and airspeed V_R are variables. Surface area of the rotor S , shape of rotor and rotor area which affect C_z are constants. As a result, total force of aerodynamical forces in microscopic area becomes the rotor thrust F_N ,

$$\begin{aligned} F_N &= 2 \int_0^R F_n dr = \int_0^R \rho (r\omega)^2 S C_z dr \\ &= \omega^2 S \int_0^R \rho r^2 C_z dr = \omega^2 A \end{aligned} \quad (8)$$

The coefficient A depending on rotor shape is

$$A = S \int_0^R \rho r^2 C_z dr \quad (9)$$

where R is a radius of rotor. Because of hardware specification, there is a limitation for the input voltages and rotors cannot rotate inverse as follows.

$$\begin{aligned} 0[\text{V}] &\leq u_r \leq 9[\text{V}] \\ 0[\text{V}] &\leq u_l \leq 9[\text{V}] \end{aligned} \quad (10)$$

3. CONTROL SYSTEM DESIGN

3.1 Structure of PID controller

In order to control the object described in (1), (2) and (3), the control inputs for making pitch angle and yaw angle follow each reference signal are designed. The reference signal of roll angle, which means desired roll angle, is calculated so that pitch and yaw angle follows their reference signals respectively. Based on the equations of

previous section, the relations between the input voltages and the output angles (r , p and y) are given as follows.

$$\begin{aligned} I_r \ddot{r} + D_r \dot{r} &= L_a A k^2 (u_2 - u_1) \\ I_p \ddot{p} + D_p \dot{p} + m g L_g \sin p &= L_m A k^2 (u_1 + u_2) \cos r \\ I_y \ddot{y} + D_y \dot{y} &= L_m A k^2 (u_1 + u_2) \sin r \end{aligned} \quad (11)$$

u_1 and u_2 are the squares of u_r and u_l respectively. The parameters in the equation (11) are replaced for simplicity as follows.

$$\begin{aligned} a_1 \ddot{r} + a_2 \dot{r} &= u_2 - u_1 \\ b_1 \ddot{p} + b_2 \dot{p} + b_3 \sin p &= (u_1 + u_2) \cos r \\ c_1 \ddot{y} + c_2 \dot{y} &= (u_1 + u_2) \sin r \end{aligned} \quad (12)$$

Each parameter is defined as,

$$\begin{aligned} a_1 &= \frac{I_r}{L_a A k^2}, \quad a_2 = \frac{D_r}{L_a A k^2}, \quad b_1 = \frac{I_p}{L_m A k^2} \\ b_2 &= \frac{D_p}{L_m A k^2}, \quad b_3 = \frac{m g L_g}{L_m A k^2}, \quad c_1 = \frac{I_y}{L_m A k^2} \\ c_2 &= \frac{D_y}{L_m A k^2} \end{aligned}$$

In (12), assuming that $F_r = \ddot{r}$, $F_p = \ddot{p}$ and $F_y = \ddot{y}$, the following equations are given.

$$\begin{aligned} F_r &= \frac{1}{a_1} \{-a_2 \dot{r} + (u_2 - u_1)\} \\ F_p &= \frac{1}{b_1} \{-b_2 \dot{p} - b_3 \sin p + (u_1 + u_2) \cos r\} \\ F_y &= \frac{1}{c_1} \{-c_2 \dot{y} + (u_1 + u_2) \sin r\} \end{aligned} \quad (13)$$

Considering that $z_r = u_2 - u_1$, $z_p = u_1 + u_2$ and $z_y = u_1 + u_2$ are given as ideal input voltages and F_p^* and F_y^* are given for z_p and z_y as ideal values, the following equations are obtained.

$$\begin{aligned} F_p^* &= \frac{1}{b_1} (-b_2 \dot{p} - b_3 \sin p + z_p \cos r) \\ F_y^* &= \frac{1}{c_1} (-c_2 \dot{y} + z_y \sin r) \end{aligned} \quad (14)$$

Because of $z_p = z_y$, the ideal roll angle r^* can be expressed from (14) as follows.

$$r^* = \tan^{-1} \left(\frac{c_1}{b_1} \frac{F_y^* + \frac{c_2}{c_1} \dot{y}}{F_p^* + \frac{b_2}{b_1} \dot{p} + \frac{b_3}{b_1} \sin p} \right) \quad (15)$$

The ideal values F_p^* and F_y^* are generated by using the following PID controller through the reference signals p_d and y_d for pitch and yaw angle. It is noticed that the reference signals p_d and y_d are constant in this paper.

$$\begin{aligned} F_p^* &= -K_{P2}(p - p_d) - K_{I2} \int (p - p_d) - K_{D2} \dot{p} \\ F_y^* &= -K_{P3}(y - y_d) - K_{I3} \int (y - y_d) - K_{D3} \dot{y} \end{aligned} \quad (16)$$

Moreover, the ideal value F_r^* to follow the ideal roll angle r^* is also given by PD control.

$$F_r^* = -K_{P1}(r - r^*) - K_{D1}(\dot{r} - \dot{r}^*) \quad (17)$$

Replacing F_r and F_p in (13) to F_r^* in (17) and F_p^* in (16), the following relations of the input voltages are given.

$$\begin{aligned} u_2 - u_1 &= a_1 F_r^* + a_2 \dot{r} = z_r \\ u_1 + u_2 &= \frac{b_1 F_p^* + b_2 \dot{p} + b_3 \sin p}{\cos r} = z_p \end{aligned} \quad (18)$$

From (18), u_1 and u_2 are obtained as follows.

$$u_1 = \frac{z_p - z_r}{2}, \quad u_2 = \frac{z_r + z_p}{2} \quad (19)$$

Because of $u_1 = u_r^2$ and $u_2 = u_l^2$, u_r and u_l are given as follows.

$$u_r = \sqrt{u_1}, \quad u_l = \sqrt{u_2} \quad (20)$$

Since the experimental device cannot carried out the reverse rotation, u_r and u_l are only positive signal. If u_r and u_l are negative signal, u_r and u_l are set to be zero.

3.2 Switching PID gains through model-based prediction and fixed ones

In the previous research[2], PID gains have been fixed for controlling the experimental device. This paper aims at improving the control performance through adaptive controller and model-based prediction. Therefore the behavior of the controlled model described in (12) with the control input (20) is virtually calculated between each control period. The calculated behavior is given in the prediction horizon which is from the time t to $t + T$ as shown in Fig.4. Because the behavior of the model is calculated at each control period, the proposed controller checks the condition of whether PID gains should be switched or not. The procedure about switching condition of PID gains is shown below. In other words, a virtual error between the output and the reference signal is calculated by the model-based prediction executed virtually.

1. The initial error E_i between the output and the reference signal is calculated at the beginning of prediction horizon.
2. The final error E_f is calculated at the end of prediction horizon.
3. The following prediction error E_p is calculated.

$$E_p = |E_i| - |E_f| \quad (21)$$

4. PID gains are switched using E_p and E_f .
5. Control inputs are calculated from the switched gains and the fixed gains. The PID gains are used in the next prediction.

For simplicity, this paper explores switching the proportional gain and the derivative gain for pitch angle only. Supposing $E_p < 0$, it seems that the actual error will become larger. In such a case, the proposed method

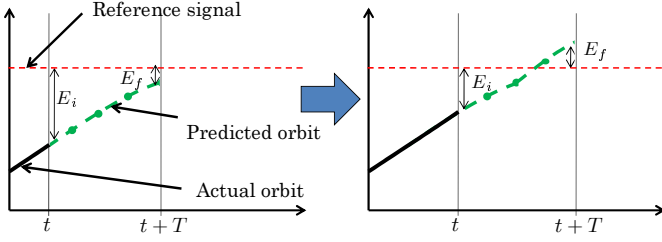


Fig. 4 Concept of model-based prediction for switching PID gains

switches the proportional gain and the derivative gain for pitch angle so as to make the actual error smaller. The following switching conditions were given by trial and error.

When $E_p > 0$ and $|E_f| > 0.157$:

$$K_{P2} = K_{P2} + \frac{0.9K_{P2}}{|K_{P2}|} e^{-t} \quad (22)$$

When $0.0785 < |E_f| < 0.3925$:

$$K_{D2} = K_{D2} + \frac{0.035K_{D2}}{|K_{D2}|} \quad (23)$$

Then the proposed controller, which consists of switching gain part and fixed gain part, can be obtained as follows.

$$\begin{aligned} F_p^* &= wF_{p_s}^* + (1-w)F_{p_f}^* \\ F_y^* &= wF_{y_s}^* + (1-w)F_{y_f}^* \\ F_r^* &= wF_{r_s}^* + (1-w)F_{r_f}^* \end{aligned} \quad (24)$$

$F_{p_s}^*, F_{y_s}^*$ and $F_{r_s}^*$ are part of switching gains calculated from (16) and (17), and $F_{p_f}^*, F_{y_f}^*$ and $F_{r_f}^*$ are part of fixed gains calculated from them. w is a weighting factor in the proposed adaptive controller. The proposed controller becomes a switching controller for $w = 1$, and a fixed controller for $w = 0$. Based on (24), the control input u_r and u_l in (20) can be calculated.

4. EXPERIMENTAL RESULT

This section gives an experimental result to show the effectiveness of the proposed method. The parameters of controlled object described in (12) are set in Table 1. In this paper, the proposed method is focused on controlling the pitch angle only because of basic investigation. The experiment has two results which are the cases of the purely switching PID controller ($w = 1$ in (24)) and a hybrid controller consisting of switching gain part and fixed gain part ($w = 0.4$ in (24)). The initial values of switching gains and the fixed gains are the same and given in Table 2. The initial values of outputs and their reference signals are given in Table 3. r^* is calculated by (15) in order to make the pitch and the yaw angles follow their reference signals. yaw_{int} means the initial value when the experiment was made and it is assumed as $yaw_{int} = 0.0$. In this experiment, the control period for the experimental device is given as 63 [ms]. The virtual sampling time

Table 1 Parameters of controlled object

a_1	=	15.9	b_1	=	43.7
a_2	=	1.02	b_2	=	1.02
c_1	=	24.7	b_3	=	36.1
c_2	=	1.84			

Table 2 Initial values of switching gains and fixed gains

	Roll($i = 1$)	Pitch($i = 2$)	Yaw($i = 3$)
K_{P_i}	5.0	5.0	5.0
K_{I_i}	0.0	0.01	0.01
K_{D_i}	0.6	0.5	4.0

Table 3 Initial values of outputs and their reference signals

	Roll	Pitch	Yaw
Initial signal [rad]	0.0	1.39	yaw_{int}
Reference signal [rad]	r^*	1.57	yaw_{int}

for the model-based prediction is set to 0.5 [s] and the prediction horizon is 25 [s], that is, the model-based prediction is executed 50 times in the control period.

In the case of $w = 1$ in (24), which means that the proposed controller becomes a switching controller, Fig.5, Fig.6 and Fig.7 show the control results of pitch angle, the input voltages for right and left motor and the switched gains (proportional gain and derivative gain) respectively. From these figures the pitch angle of experimental device converges to the constant value while switching the proportional gain and the derivative gain. In the case of $w = 0.4$ in (24), which means that the proposed controller consists of switching gain part and fixed gain part, Fig.8, Fig.9 and Fig.10 show the pitch angle, the input voltages and the switched gains. From these figures, it can find that the pitch angle does not converge even if the proportional gain and the derivative gain are switched.

5. CONCLUSION

In our previous research, switching PID controller was applied to the underactuated flying object model and the effectiveness was confirmed on numerical simulation. In order to check the practical ability of the proposed adaptive PID controller which consists of switching gains and fixed ones, the proposed method was applied to the experimental device. The effectiveness of the proposed method was shown by the experimental result.

As future works, there is an investigation into the switching condition for various reference signals and the relation between the virtual sampling time and the prediction horizon for model-based prediction. Moreover

the proposed method should be improved aiming at the quick convergence to reference signal.

REFERENCES

- [1] S. Mizokami, K. Yoshikawa, A. Yanou, M. Minami and T. Matsuno, *Adaptive Predictive Control System for Underactuated Flying Object Experimental Device*, Proc. of the 2015 JSME Conference on Robotics and Mechatronics, 2A2-G08, 2015.
- [2] K. Yoshikawa, A. Yanou and M. Minami, *Position/Orientation Control of an Underactuated Flight Object Based on Two Degree-of-Freedom PID Control*, Proc. of SICE Annual Conference, pp.1204-1209, 2012.
- [3] M. Deng, A. Inoue and T. Shimizu, *Combined Attitude Control of an Underactuated Helicopter Experimental System*, Proc. of UKACC International Conference on Control 2008, 2008.
- [4] M. Deng, A. Inoue, H. Yu, T. Shimizu, *Combined attitude control application of an underactuated helicopter experimental system*, Int. J. Advanced Mechatronic Systems, Vol.1, No.4, pp.280-287, 2009.
- [5] A. Yanou, K. Yoshikawa, S. Mizokami, M. Minami and T. Matsuno, *Switching PID Control for an Underactuated Flying Object Through Model-Based Prediction*, Proc. of IEEE 10th Asian Control Conference, 2015.
- [6] M. Deng, A. Inoue, T. Kishida, and N. Ueki, *Modeling and control of an underactuated helicopter experimental system*, Proc. of the 26th Chinese Control Conference, pp.648-651, 2007.
- [7] A. Inoue, M. Deng, T. Shimizu and T. Harima, *Experimental study on attitude control system design of a helicopter experimental system*, Proc. of International Control Conference (ICC2006), 2006.
- [8] A. Kojima, T. Ohtsuka, *An Introduction to Model Predictive Control*, Journal of the Society of Instrument and Control Engineers, Vol.42, No.4, pp310-312, 2003.

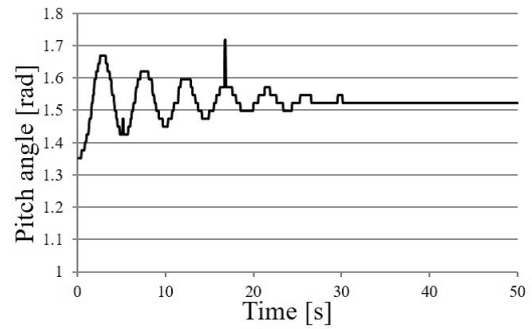


Fig. 5 Pitch angle by the proposed method ($w = 1$)

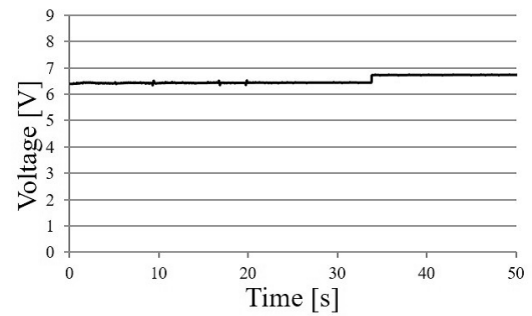
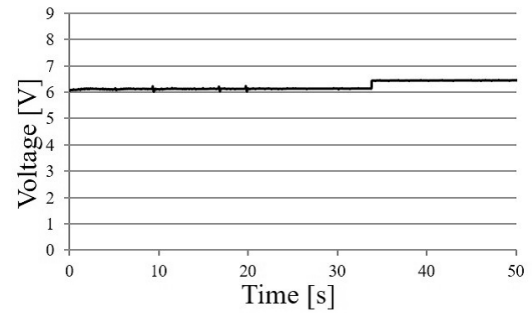


Fig. 6 Input voltages ($w = 1$, upper:right motor, lower:left motor)

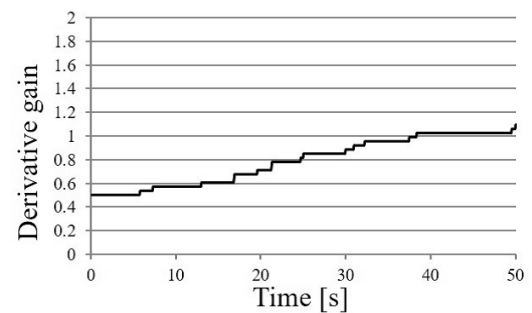
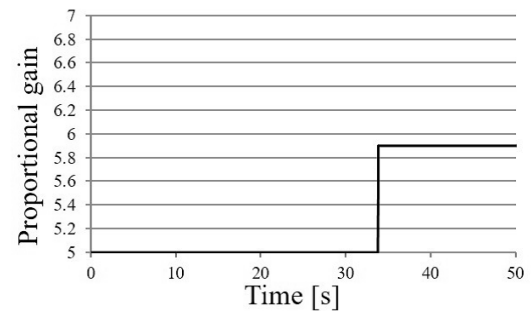


Fig. 7 Switched gains ($w = 1$, upper:proportional gain, lower:derivative gain)

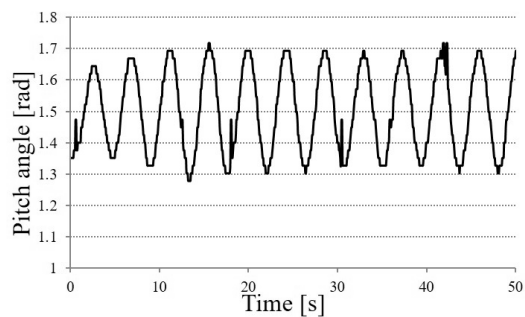


Fig. 8 Pitch angle by the proposed method ($w = 0.4$)

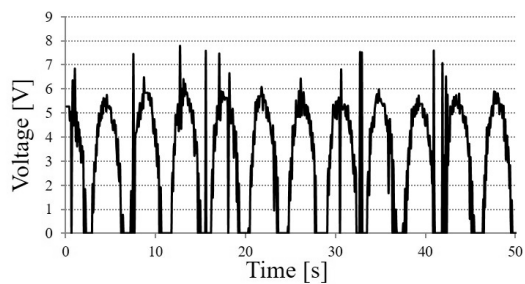
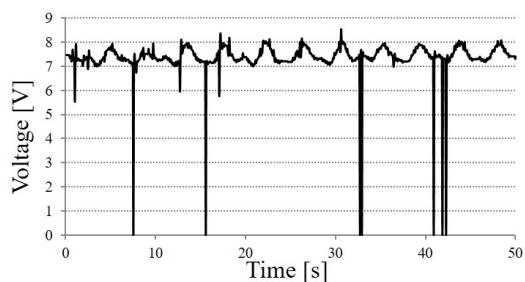


Fig. 9 Input voltages ($w = 0.4$, upper:right motor, lower:left motor)

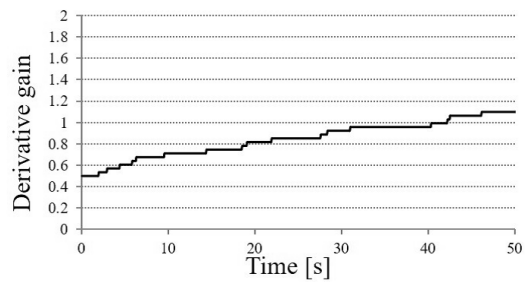
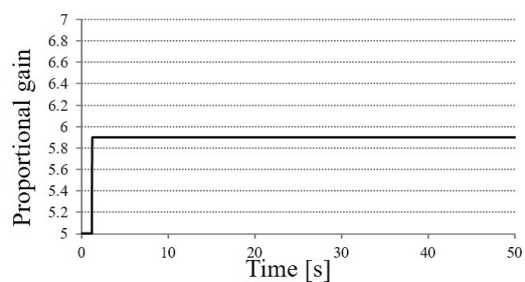


Fig. 10 Switched gains ($w = 0.4$, upper:proportional gain, lower:derivative gain)